One-step pathogen specific DNA extraction from whole blood on a centrifugal microfluidic device†

Yoon-Kyoung Cho, Jeong-Gun Lee,* Jong-Myeon Park, Beom-Seok Lee, Youngsun Lee and Christopher Ko*

Received 6th November 2006, Accepted 22nd January 2007 First published as an Advance Article on the web 15th February 2007

DOI: 10.1039/b616115d

We report a fully integrated, pathogen-specific DNA extraction device utilizing centrifugal microfluidics on a polymer based CD platform. By use of the innovative laser irradiated Ferrowax microvalve (LIFM) together with the rapid cell lysis method using laser irradiation on magnetic particles, we could, for the first time, demonstrate a fully integrated pathogen specific DNA extraction from whole blood on a CD. As a model study, DNA extraction experiments from whole blood spiked with Hepatitis B virus (HBV) and *E.coli* were conducted. The total process of the plasma separation, mixing with magnetic beads conjugated with target specific antibodies, removal of plasma residual, washing and DNA extraction was finished within 12 min with only one manual step, the loading of $100~\mu L$ of whole blood. Real-time PCR results showed that the concentration of DNA prepared on a CD using a portable sample preparation device was as good as those by conventional bench top protocol. It demonstrates that our novel centrifugal microfluidics platform enables a full integration of complex biological reactions that require multi-step fluidic control.

1. Introduction

There have been significant advances in lab-on-a-chip development for biomedical applications during the last decade. ¹⁻⁶ However, the majority of the reports so far have used purified DNA or cells in buffer solutions as an input sample. On the other hand, the practical applications in clinical diagnostics require processing of complex fluids such as whole blood, urine, and saliva. Owing to the complex nature of the sample and the many operational steps, most of the sample preparation steps still rely on time-consuming traditional bench top methods. As a result, development of rapid and efficient on-chip sample preparation for "real" sample analysis remains as a major bottleneck for the realization of the true lab-on-a-chip. ⁷⁻¹⁵

Recently we reported a novel cell lysis method, laser-irradiated magnetic bead system (LIMBS). Addition of magnetic beads to the pathogen containing solution accelerated the heating speed. Therefore, DNA from various types of pathogens, including both Gram-negative and Gram positive bacteria and hepatitis B viruses, was effectively extracted by simply applying 40 s of laser (808 nm, 1.0 W) irradiation. However, direct DNA extraction using LIMBS from raw samples such as whole blood and the concentration of cells or DNA were not possible.

In this paper, we report a fully integrated pathogen specific DNA extraction device utilizing centrifugal microfluidics on a

Bio Device Research Laboratory, Samsung Advanced Institute of Technology, P.O. Box 111, Suwon, 440-600, Korea. E-mail: biogun.lee@samsung.com; chrisko@samsung.com polymer based CD. The design principles are shown schematically in Fig. 1A. As a model study, DNA extraction from whole blood spiked with HBV or $E.\ coli$ was conducted using a CD pre-loaded with reagents, antibody-coated magnetic beads and washing buffer. The total process of plasma separation, mixing with magnetic beads conjugated with HBsAg specific antibodies, removal of plasma residual, washing, and DNA extraction was finished within 12 min with only one manual step of loading 100 μ L of whole blood to start the assay.

The "Lab-on-a-CD" platform in which the centrifugal pumping is the basic physical principle to transfer liquid in microfluidic structures was first investigated by Madou's group in 1998. ^{17–19} Various fluidic functions such as valving, ^{17,20–23} metering, ²¹ mixing, ²⁴ sample switching, ²⁵ and separation ²⁶ have been demonstrated on CD type platforms. ¹⁹ The examples of application include cell lysis combined with polymerase chain reaction (PCR), ²³ two-point calibration for the ion sensor, ²⁷ enzyme-linked immunoassay, ^{28,29} cell lysis, ³⁰ high-throughput screening, ²⁰ and alcohol assay from whole blood. ³¹

The majority of centrifugal microfluidic platforms have utilized either hydrophobic or capillary valves. The fabrication and the simultaneous actuation of multiple valves were relatively simple. However, for the robust control of the valving operation, fine tuning of the spin speed, as well as the local surface properties or dimensions of the microchannels, were required. Furthermore, these valves can function only as opening valves, *i.e.*, from normally closed state to open state, not *vice versa*. As a result, only a limited number of diagnostic tests that do not require complex fluidic design have been developed on a CD platform and launched onto the market. ^{29,32–34}

We have demonstrated an innovative laser irradiated ferrowax microvalve (LIFM) that is based on phase transition of ferrowax, parrafin wax embedded with 10 nm sized iron

[†] Electronic supplementary information (ESI) available: Schematic diagram of the CD fabrication and microfluidic layout, spin program for the DNA extraction on a CD using TS-LIMBS, captions to movie files and movie files 1 and 2. See DOI: 10.1039/b616115d

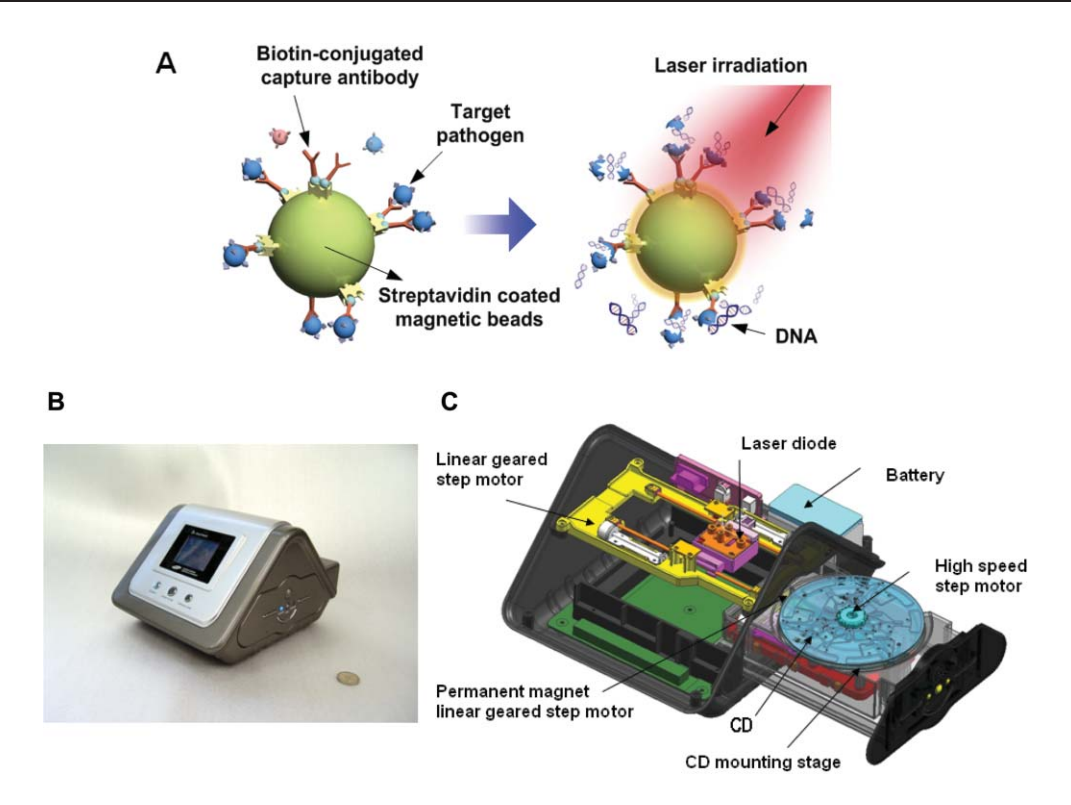


Fig. 1 (A) Schematic diagram of the reaction principle. The magnetic beads conjugated with target specific antibody are mixed with sample solution. Target pathogens are selectively captured on the magnetic beads and the waste materials such as plasma residue are washed away. Simple irradiation by laser (808 nm, 1.5 W) for 30 s could effectively extract PCR-ready DNA from captured target pathogens. (B) A photo image of the portable device to operate a lab-on-a-disc for rapid DNA extraction from whole blood using target separation and laser-irradiated magnetic bead system (LIMBS). A single laser diode was used not only to operate multiple laser irradiated ferrowax microvalves (LIFM) but also to extract DNA from pathogens. (C) Schematic diagram showing the inside of the portable lab-on-a-disc device. A laser diode is mounted on a linear geared step motor. A permanent magnet is located on the other linear geared step motor located under the CD mounting stage. A high speed step motor is used to run the spin program.

oxide nanoparticles.³⁵ Compared with conventional phase change based microvalves, the control of multiple microvalves was made simple by using a single laser diode instead of multiple embedded micro-heaters.^{15,36} Furthermore, LIFM is not very sensitive to rotation speed or surface properties. Both normally closed (NC)–LIFM and normally opened (NO)–LIFM were demonstrated and various fluidic functions, such as valving, metering, mixing, and distribution, were demonstrated using centrifugal microfluidic pumping. In addition, the response time to open the channel by melting the wax was dramatically reduced from 2–10 s to less than 0.5 s because the laser beam effectively heats the nanopaticles embedded in the paraffin wax matrix.^{15,35,37}

In this report, a single laser diode was used for dual purposes: for the multiple LIFM control as well as for the cell lysis. Because the laser beam is effectivley absorbed on magnetic beads or iron oxide nanoparticles and the heat is generated very rapidly, both the response times to extract DNA from pathogens and to operate microvalves were dramatically reduced. Furthermore, a hand-held type sample preparation device was developed as shown in Fig. 1C. Since a step motor and a laser diode are the key components for full control of microfluidics on a lab-on-a-disc, the device size is very compact $(213.0 \times 272.3 \times 165.8 \text{ mm}, 1865g)$.

Using the innovative LIFM together with the pathogen specific magnetic particles, we could, for the first time to the

best of our knowledge, demonstrate a fully integrated pathogen specific DNA extraction from whole blood on a portable lab-on-a-disc device. It shows that our novel centrifugal microfluidic design enables a full integration of biological reactions that require complex batch mode microfluidic controls.

2. Materials and methods

2.1. Micro-valve operation on a CD

The ferrowax valve is made of a nanocomposite materials composed of 50% of paraffin wax ($T_{\rm m}$: 50–52 °C, Fluka Chemie GmbH) and 50% ferrofluids (10 nm sized iron oxide nanoparticles dispersed in oil; APG 314, Ferrotec Inc., CA, USA). The detailed procedure of the fabrication and characterization of LIFM have been previously reported. ³⁵

2.2. Instrumentation

An experimental set-up for the centrifugal microfluidic control has been designed. In addition to the detailed description of the test vehicle previously reported, ³⁵ a Nd–Fe–B magnet (JungWoo, Korea) is attached on a linear geared stepping motor under the CD mounting stage to control the position of the other Nd–Fe–B magnet included on the bottom of the CD. As shown in Fig. 1B, a hand-held type sample preparation

device was assembled using a high power laser diode (BS808T2000C-MOUNT, Best-Sources Industry (HK) Co. Ltd, China) and high speed step motor (19TM-J802, Minebea Co. Ltd). The energy source of the device is 6 lithium ion battery packs (3.6 V 2200 mAh, LG 18650, LG CHEM, Korea). A microprocessor (PIC16F74, Microchip Technology Inc., USA) and a main control board (Analog Research System, Korea) are used to regulate laser power, the high speed step motor, and the linear geared step motor for the positioning of the laser diode and permanent magnet. The spin program can be downloaded from a PC and stored in the EEPROM of the device *via* RS-232 communication. The laser operation in the portable device is shown in Movie file 1 in the Electronic Supplementary Information†.

As is shown in Fig. S1 in the ESI \dagger , both the top and bottom layers of the CD are made of polycarbonate (PC) plates and bonded with a double sided adhesive tape (Flexmount DFM 200 Clear V-95 150 POLY H-9 V-95 4, FLEXcon Inc., MA, USA). The inlet holes and microfluidic layouts were produced by a conventional Computer Numerical Control (CNC) machine (Sirius 550, Hwacheon Inc., Seoul, Korea). The top plate has inlet holes and the bottom plate has chambers with a depth of 3 mm. The microfluidic channels to transfer liquids between reservoirs are formed in the middle layer. The widths of the channels were 1 mm and the depth of the channel was 100 μ m because the thickness of the tape was 100 μ m. As is shown in Fig. S1 \dagger , each CD has three identical DNA extraction units.

2.3. Target specific concentration and DNA extraction using laser irradiation

The DNA extraction process is composed of plasma separation, mixing, with magnetic beads conjugated with target specific antibodies, washing of the magnetic beads, and lysis using laser irradiation.

As a model system for virus concentration and DNA isolation, HBV serotype ayw, kindly provided by Professor Wang-Shik Ryu (Department of Biochemistry, Yonsei University, Korea), was used. HBV solution (3 \times 10⁶ copies mL⁻¹) was spiked with human whole blood with a volume ratio of 1:2. The final HBV concentration of the sample was 10^4 – 10^6 copies mL⁻¹.

In addition, as a model system for bacteria concentration and DNA extraction, *E. coli* (K12, ACCT 25404) was cultured at 37 °C with vigorous aeration in brain heart infusion (BHI) medium to an exponential phase (OD 600 = 0.5–1.0). The bacterial cells were harvested by centrifugation and washed twice with 3 ml of phosphate-buffered saline (PBS). The cells were re-suspended in PBS (cell density; 1×10^5 cells μL^{-1}).

In order to prepare antibody coated magnetic beads, $10 \mu g$ of the primary biotinylated antibodies (Virostat, 1817 (HBV), 1007 (E. coli), USA) were added to the $100 \mu L$ of pre-washed streptavidine modified magnetic beads (Dynabeads, MyOne Streptavidin C1, $100 \mu L$, diameter of $1 \mu m$, $10 mg mL^{-1}$, $7-12 \times 10^9$ beads mL^{-1}) and incubated for over 30 min at room temperature. The tube was placed in a magnet holder for 2 min and the supernatant was discarded. The beads were washed twice with a washing buffer (PBS without Ca^{2+} and

 ${\rm Mg}^{2+}$ with 0.1% BSA, pH 7.4.). The pre-coated beads are resuspended in 100 μL of the buffer.

Isolation of the pathogen was carried out by adding $100~\mu L$ of pre-coated beads to the $100~\mu L$ of sample, whole blood spiked with *E. coli* $(10^4 – 10^6~\text{cell}~\mu L^{-1})$ or HBV $(10–10^3~\text{copies}~\mu L^{-1})$, followed by incubation for 3–20 min with gentle tilting and rotation. The reaction tube was placed in a magnet holder for 2 min and the supernatant was washed away. The beads were washed with $100~\mu L$ of the deionized water twice. The lysis step was done by applying a laser with a radiation power of 1.5 W for 30 s using a single laser diode (808 nm, L8828-72, Hamamatsu Photonics, Japan).

In order to quantify the amount of HBV DNA, we used real-time PCR (TMC 1000, SAIT, Korea)³⁸ and the PCR product was quantitated using Agilent Bioanalyzer 2100 for verification. The following primers and Taqman probe were used for the real-time PCR of HBV: forward primer, 5'-AGTGTGGATTCGCACTCCT-3'; reverse primer, 5'-GAGTTCTTCTTCTAGGGGACCTG-3'; and TaqMan probe 5-FAM-CCAAATGCCCCTATCTTATCAACACTT-CC-TAMRA-3. The primer set for the core region detection was designed to amplify 118 bp fragment in a core region originally by Chen *et al.*,³⁹ against a highly conserved region among 25 published HBV genome sequences in GenBank and EMBL, representing genotypes A–F.

PCR amplification was carried out using Taq polymerase (Solgent, Korea) for 40 cycles (95 °C for 2 min to pre-denature, 95 °C for 15 s to denature, 58 °C for 60 s to anneal and extend). The PCR was performed by real-time PCR (TMC 1000, SAIT, Korea)³⁸ with a total volume of 1 μ L reaction mixture containing 10X PCR buffer (2.5 mM MgCl₂, Solgent. Co. Ltd, Korea), 0.9 μ M of forward and reverse primers, and also 0.4 μ M of TaqMan probe (Bioneer, Korea), 200 μ M dNTP mixture and 0.1 U μ L⁻¹ Taq polymerases (Solgent, Korea). After the lysis step of the laser irradiation for 30 s, the magnetic beads were driven to one side using the permanent magnet, and the DNA solution was taken out and followed by the real-time PCR detection.

3. Results and discussion

3.1. Bacteria concentration and DNA extraction using laser irradiation

The magnetic beads are used for dual purposes. First, they are modified with pathogen specific antibodies and thus act as a mediator for a pathogen specific cell separation and concentration. Second, they act as micro-heaters for rapid heat transfer. The 808 nm laser is not absorbed by water molecules but effectively absorbed by the magnetic beads dispersed in solution. As a result, the heating speed is ultra-fast and the cell

lysis step could be dramatically shortened. Furthermore, a large volume of lysis buffer is not necessary, which is another favorite characteristic of the miniaturization.

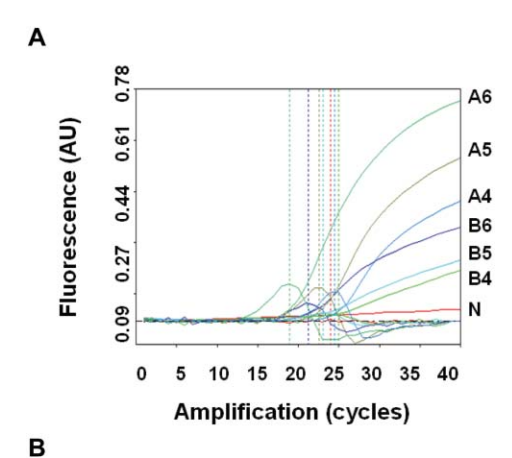
Furthermore, in our design of the lab-on-a-disc system shown in Fig. 1B, a single laser diode is also used for dual purposes: a non-contact type heating source for the control of multiple ferrowax valves as well as for the rapid cell lysis.

First, the comparison experiment of DNA concentration prepared by the proposed target separation and laserirradiated magnetic bead system (TS-LIMBS) and the previously reported LIMBS¹⁶ were conducted. As shown in Fig. 2A, the crossing point (Cp) values from the real-time PCR results of the DNA prepared by using the TS-LIMBS (A6, A5, A4) were smaller than those with the sample prepared by the previously reported LIMBS (B6, B5, B4).

Cp is defined as the cycle number at which the fluorescence passes the fixed threshold. It has been reported that 10-fold differences in the template DNA concentration result in 3.32 cycle differences in Cp when PCR the efficiency is 100%. 38,39

Because the initial sample volume was 100 µL and the final elution volume was 10 µL, about 10 times the concentration is expected assuming 100% preparation efficiency. The experimental results showed the concentration was increased about 2-7 times by using TS-LIMBS, depending on the initial cell concentration.

In order to measure the capture efficiency of the antibody coated magnetic bead for specific target, each concentration of the initial bacteria solution (I), left-over bacteria in the binding



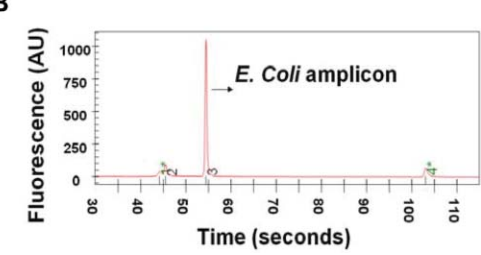


Fig. 2 Experimental results of bacteria concentration and DNA extraction. (A) Real-time PCR results of the DNA prepared by using the TS-LIMBS (A6, A5, A4) and previously reported LIMBS (B6, B5, B4). The initial bacteria concentrations were 10⁶ (A6, B6), 10⁵ (A5, B5), 10^4 (A4, B4) cell μL^{-1} and a negative control (N). (B) The amplified PCR products were taken out from the 1 µL micro PCR chip and analyzed using Agilent Bioanalyzer 2100.

Table 1 Bacteria capture efficiency

E. coli concentration/cell μL ⁻¹	Capture efficiency (I-B-W)/I × 100 (%)	CV (%) (n = 4)	
10 ⁵ 10 ⁴	93.4	0.2	
10^{4}	87.6	0.9	
10^{3}	92.5	1.6	

buffer after the binding experiment (B), and bacteria in the washing buffer (W) were measured by using colony counting methods using Petrifilm (3 M). For the measurement of each solution, 3 replicates of 3 different concentrations of serially diluted sample (ranging from 10 to 1000 cells) were used for the colony counting methods. The capture efficiency was calculated by $(I-B-W) I^{-1} \times 100\%$. As is shown in Table 1, the capture efficiency was about 90% at the concentration ranges studied $(10^4-10^6 \text{ cell } \mu\text{L}^{-1})$.

The concentration experiments using E. coli spiked in whole blood were conducted as shown in Table 2. In this case, the colony counting methods were not accurate because the bacteria begin to die when they are mixed with whole blood. When whole blood was used, the LIMBS method could not prepare PCR-ready DNA. When the pure buffer was used, the addition of the target separation step decreased Cp by 1.65 cycles. The initial E. coli concentration calculated using a calibration curve (data not shown) showed that the DNA concentration was increased by about 3.4 times when the target separation and concentration step was added. It is note worthy that the Cp values from the DNA solution prepared from the whole blood using the TS-LIMBS method were as good as those from pure PBS buffer.

3.2. Virus concentration and DNA extraction using laser irradiation

DNA isolation from whole blood spiked with HBV was conducted using the TS-LIMBS. In order to find the optimum condition of the TS-LIMBS method to be integrated on a CD platform, the effect of the particle size, surface property, the concentration of the magnetic beads, the binding time, the volume of the washing buffer and the number of the washing steps have been investigated.

As is shown in Fig. 3A, the C1 type of the beads (Dynabeads MyOne Streptavidin C1, diameter 1 µm, binding capacity of biotinylated Ig 15–20 μg mg⁻¹, hydrophilic, carboxylic acid beads) showed the best results compared with other kinds of beads with larger sizes, e.g., M-280 (Dynabeads M-280 Streptavidin, diameter 2.8 µm, binding capacity of biotinylated Ig 5-10 μg mg⁻¹, hydrophobic, tosyl activated beads) and

Table 2 Real-time PCR detection of bacteria (E. coli, 10^5 cell μL^{-1}) from whole blood. The volume ratio of the bacteria solution and the whole blood was 1:2. In the table, X means that no PCR amplicon was obtained

E. coli in—	Method	Ср	PCR product conc./ng μL ⁻¹
PBS Whole blood PBS Whole blood	TS-LIMBS TS-LIMBS LIMBS LIMBS	19.40 19.43 21.05	20.3 17.9 15.3

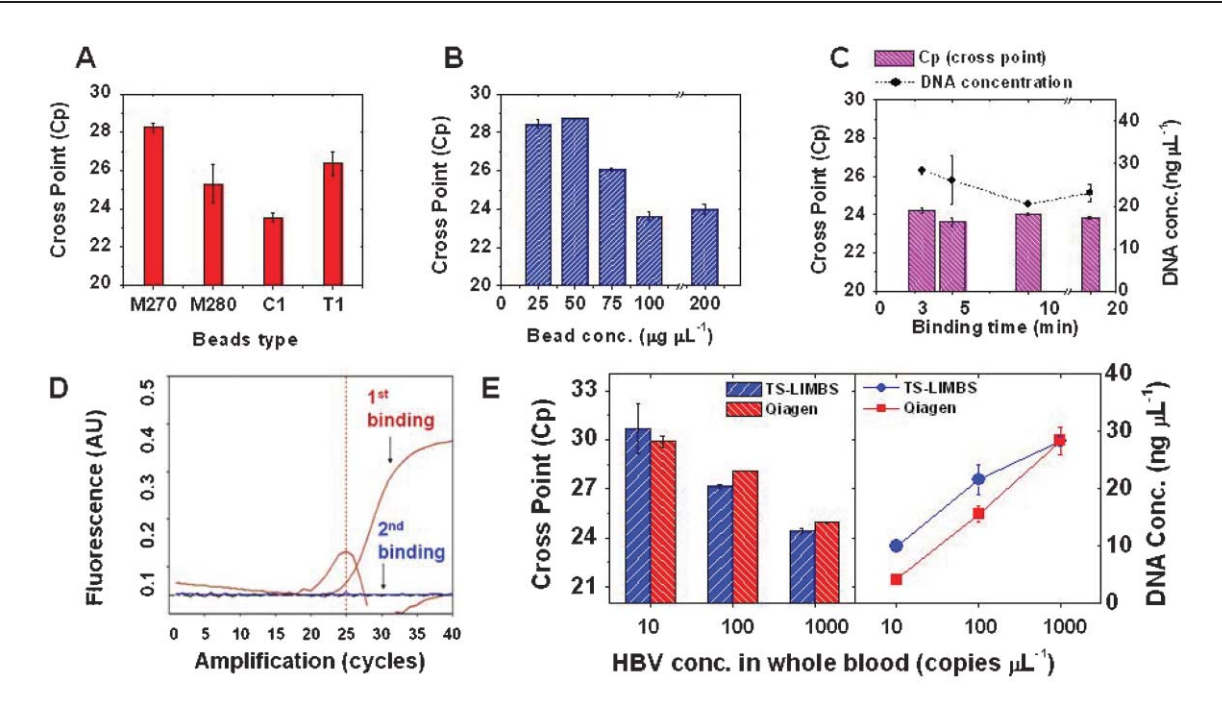


Fig. 3 Key factors for the efficiency of the DNA preparation using TS-LIMBS were investigated by real-time PCR and measurement of the concentration of the PCR amplicon using Agilent Bioanalyzer 2100. Effects of the magnetic bead type (A), the bead concentration (B), and the binding time (C) on the real-time PCR results were investigated. (D) To see the capture efficiency of the antibody conjugated magnetic beads, binding experiments were carried out twice using the virus solution. The antibody coated magnetic beads capture almost all of the virus in the first binding experiment and there was no PCR amplicon from the second binding experiments (E). The DNA preparation efficiency of our TS-LIMBS was compared with the results obtained by using a commercial virus DNA preparation kit (Qiagen, QIAamp MinElute virus vacuum kit, 57714). The blue and red symbols represent the results obtained by using TS-LIMBS and Qiagen kits, respectively. Both real-time PCR results and DNA concentration measured by TMC-1000 and Agilent Bioanalyzer 2100, respectively, showed that the newly proposed TS-LIMBS method is at least as good as the commercially available virus DNA preparation kit.

M-270 (Dynabeads M-270 Streptavidin, diameter 2.8 μm, binding capacity of biotinylated Ig 5–10 μg mg⁻¹, hydrophilic, carboxylic acid beads) or hydrophobic and tosyl activated beads, *e.g.*, T1 (Dynabeads Dynabeads MyOne Streptavidin T1, diameter 1 μm, binding capacity of biotinylated Ig 40–50 μg mg⁻¹, hydrophobic, tosyl activated beads).

Because we used the same mass concentration of the beads, the surface area of the beads with smaller sizes was larger and thus the binding capacity of the biotin labelled antibody was larger. In addition, as we previously reported, carboxylated beads showed superior protein removal function compared with other amine modified or polystyrene beads.

As is shown in Fig. 3B, the larger concentration of the magnetic beads resulted in better PCR products up to 100 $\mu g \ \mu L^{-1}$. Because we used 100 μL of C1 beads (10 mg mL $^{-1}$) and the final lysis chamber volume was 10 μL , the bead concentration in lysis chamber was 100 $\mu g \ \mu L^{-1}$. We previously reported that the higher the magnetic bead concentration the higher the cell lysis efficiency in the range of the magnetic beads concentration from 0 to 90 $\mu g \ \mu L^{-1}$.

The commercial sample preparation kits using magnetic beads usually recommend the incubation time of 20 min for the binding of antibodies on the bead surfaces. However, as shown in Fig. 3C, when we varied the binding time from 3 to 20 min the lysis efficiency was not affected much and thus the binding time of 3 min was used thereafter.

The measurement of the capture efficiency was not trivial for the virus sample because virus culture was not possible. Instead, we added the antibody conjugated magnetic beads to the virus solution twice and amplified DNA from each step. As is shown in Fig. 3D, most of the virus was captured in the first binding step and no PCR amplicon was obtained in the second binding experiment.

The DNA preparation efficiency of our TS-LIMBS was compared with a commercial kit (Qiagen, QIAamp MinElute virus vacuum kit, 57714). The MinElute virus vaccum kit requires 500 μL of serum or plasma sample and takes over 1 hour, with many manual steps involving adding various buffers. Our TS-LIMBS method uses only 30 μL of serum or plasma sample and takes 12 min with only one step.

Though the initial sample volume requirements are different, in order to make a comparison we used the same concentration factor, *i.e.*, the ratio of the initial plasma sample volume to the final volume of the DNA solution. For the Qiagen preparation kit, $100~\mu L$ of plasma sample was mixed with $400~\mu L$ of PBS buffer and the final elution volume was $33~\mu L$. Because $30~\mu L$ of plasma was used, and the final volume was $10~\mu L$ in the TS-LIMBS method, the concentration factor was the same.

As is shown Fig. 3E, the real time PCR results prepared by the proposed TS-LIMBS method were at least as good as a commercially available kit (Qiagen, QIAamp MinElute virus vacuum kit, 57714). The limit of the detection was 10 copies μL^{-1} for both of the preparation methods. It is noteworthy that the cut-off range for the HBV DNA test in current clinical diagnostics is 100 copies μL^{-1} .

3.3. CD designs and spin program

As is shown in Fig. 4, a microfluidic layout was designed to fully integrate the TS-LIMBS method on a CD. Table S1† shows the spin program at each operation step. The images shown in Fig. 4 were obtained during the rotation using the CCD camera and strobe light as previously described.³⁵

First, 100 μ L of human whole blood spiked with HBV solution (10–10³ copies μ L⁻¹, 66% blood composition) and 100 μ L of the antibody conjugated magnetic bead solution (10 mg mL⁻¹) and 200 μ L of washing buffer (deionized water) were added to the blood chamber, bead chamber, and washing buffer chamber, respectively, as shown in Fig. 4A. The plasma was separated by spinning the CD at 60 Hz for 120 s.

The dimension of the plasma separation channel was designed so that the volume of the plasma located where the distance from the center, r, is smaller than that of the first valve is 30 μ L. The metered plasma is transferred to the mixing

chamber by spinning the CD at 60 Hz for 5 s as soon as the NC-LIFM 1 is melted by applying the laser for 1 s. During spin No. 1 for the plasma separation, the magnetic beads are also sedimented.

Using the same method of the valve operation, the magnetic beads solution is transferred to the mixing chamber as shown in Fig. 4B. The mixing of magnetic beads and plasma solution was effected by alternate spining of the CD at the spin condition that provokes maximum vortexes, as shown in Fig. 4C: maximum spin speed of +9 to -9 Hz and acceleration of 60 Hz s⁻¹. Using the proposed optimum spin program, the effective mixing was obtained within 1 s. In order to have enough binding time, the alternate spinning was continued for 4 min.

After the mixing step, the beads are sedimented by spining the CD at 60 Hz for 60 s. Next, the plasma residual is removed to the waste chamber by opening the NC-LIFM 3. Then, the NO-LIFM 4 is closed to seal the channel to the waste chamber

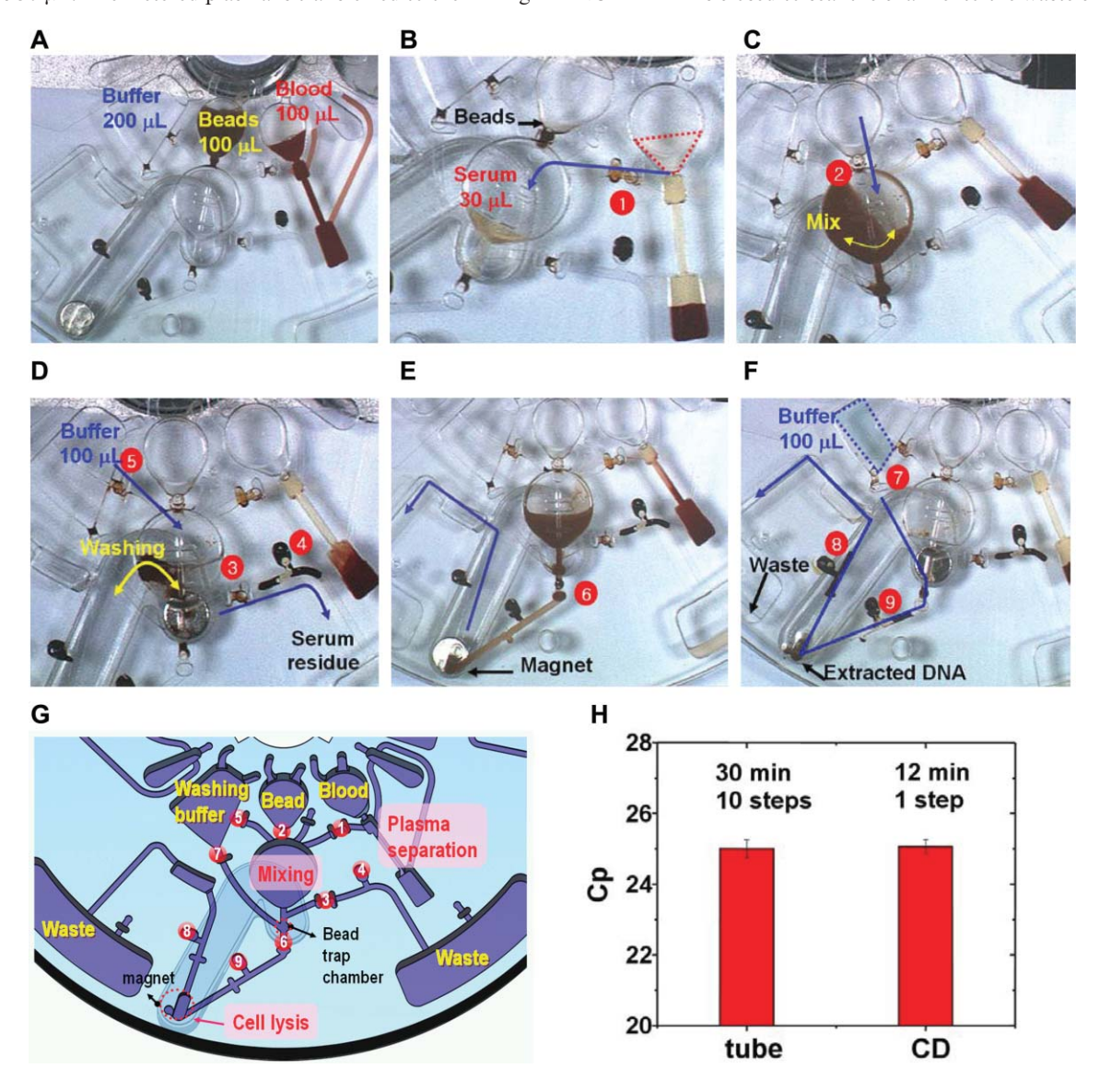


Fig. 4 (A–F) CCD images captured at each spin step using the spin program shown in Table S1†. (G) CD design showing the detailed microfluidic layout and functions. The number indicates the order of the LIFM operation. (H) Real time PCR results from DNA prepared TS-LIMBS by tube based manual method and by the fully automated method on a CD.

as shown in Fig. 4D. Now the volume of the bead solution in the bead trap chamber is only 2.5 μL .

By opening the NC-LIFM 5, 100 μ L of washing buffer is transferred to the mixing chamber as shown in Fig. 4D. For the efficient washing, the permanent magnet on the magnet rail cap attached on the bottom of the CD is moved to the mixing chamber to attract and move the sediment beads to the mixing chamber. Otherwise, the tightly packed beads in the small bead trap chamber after the spin step 5 were not effectively moved to the lysis chamber. The detailed mechanism to move the magnet on the rotating CD is described in Section 3.4.

The target pathogen captured beads in washing buffer are now moved to the lysis chamber. At this time, the permanent magnet is located at the bottom of the lysis chamber, as shown in Fig. 4E. After repeating the washing step once more, the lysis chamber is sealed by irradiation by the laser beam on NO-LIFM 8 and NO-LIFM 9, as shown in Fig. 4F. Finally, the lysis step is carried out by applying the laser for 30 s and the DNA solution is transferred to the PCR chip for real-time PCR. (See Movie file 2 in the ESI† for the full process of DNA extraction on a CD.) Fig. 4G shows the detailed microfluidic layout and functions. The numbers in LIFM position indicate the order of the LIFM operation.

Fig. 4H shows that the DNA extraction efficiency was about the same no matter which manual tube-based method or fully automated CD was used. The total process is automatically controlled by custom-designed software and takes less than 12 min.

3.4. Control of the location of magnetic beads on a rotating CD using a magnet moving rail

Magnetic particles have been used in many molecular biology areas either with manual operation or in automated large sized instruments. Although simple immunoassays or blood tests have been tried on a CD platform, ^{19,29} it is the first trial to integrate magnetic beads based assay on a CD platform.

In order to control the location of the magnetic beads on a rotating CD, two permanent magnets (Nd–Fe–B Magnet, JungWoo, Korea) were used. One magnet was inserted on a magnet moving rail attached on the bottom of the CD. The other magnet was fixed on the CD mounting stage and the position could be controlled by using a linear geared step motor. Both magnets were aligned to be attractive.

Depending on the direction and spin speed of the rotating CD and the position of the magnet at the bottom, the location of the magnet inserted on the CD could be determined. For example, when the CD is rotated with a spin speed of 3 Hz to the clockwise direction, the magnet moves to the counterclockwise direction and stays at the position A, as schematically shown in Fig. 5A. When the spin speed is increased to 8 Hz, the magnet moves to the position B. On the other hand, if the CD spins to the counter clockwise direction with a spin

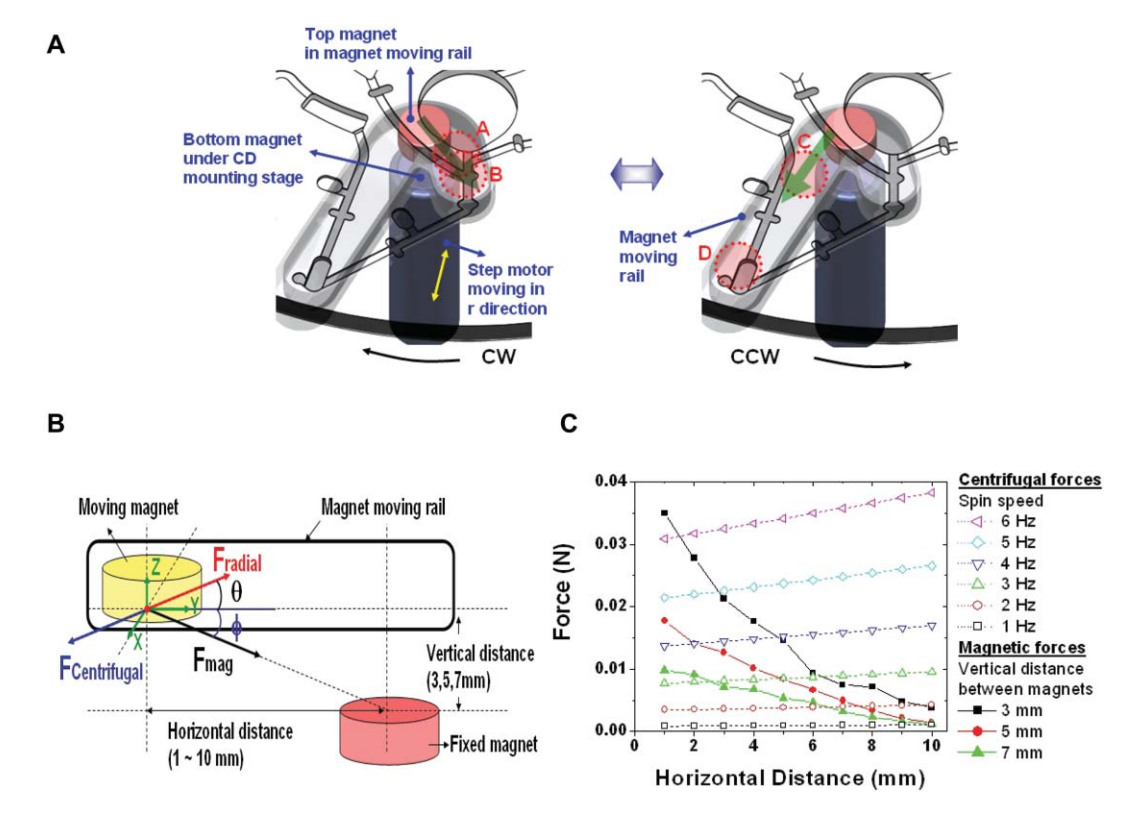


Fig. 5 (A) The principle of the control of the location of the magnet inserted on a CD (indicated by yellow circle) using a magnet moving rail cap. The red circle indicates the position of the fixed bottom magnet under the CD mounting stage. Depending on the direction and spin speed of the rotating CD and the position of the magnet at the bottom, the location of the magnet inserted on the CD is determined. (B) The radial component of the magnetic force between the fixed magnet under the CD and the moving magnet on the rotating CD, $F_{\rm radial}$ is balanced with the centrifugal force. (C) The magnetic force is dependent on the vertical and horizontal distance between magnets. (D) The radial components of the magnetic forces and the centrifugal forces were calculated as a function of the horizontal distances between the two Nd–Fe–B magnets.

speed of 8 Hz the magnet moves to position C, and if the spin speed is larger than 10 Hz, the centrifugal force wins over the magnetic force and thus the magnet moves to the position D.

At small spin speed, the magnet inserted on a rotating CD is moved to the position where the bottom magnet is located; the magnetic force is larger than the centrifugal force. However, *vice versa*, if the spin speed is fast and the direction of the spin is clockwise, the magnet moves to the counter-clockwise direction due to the inertial force. If the spin speeds are too fast, *i.e.*, the centrifugal force is larger than the magnetic force, the magnet moves to the radial direction to the end of the magnet-moving rail. By using this mechanism of force balance between the magnetic force and centrifugal force, the location of the magnet on a rotating CD could be controlled.

The novel mechanism to control the location of magnets on a rotating CD was effectively used in the DNA extraction CD. For example, we could rapidly move the magnetic beads to the mixing chamber for effective washing and also trap them in the lysis chamber.

In order to further investigate the force balance between the magnetic force and the centrifugal force, we have calculated the magnetic force using a commercial numerical simulation package CFD-ACE⁺ (ESI Group).

The magnetic forces were calculated using the actual CD geometry shown in Fig. 4. The centrifugal force given as

$$F_{\rm cent} = mr\omega^2 \tag{3}$$

and is balanced with radial component of the magnetic force given as

$$|F_{\text{radial}}| = |F_{\text{mag}}| \times \cos(\theta) \times \cos(\phi)$$
 (4)

where m is the mass of the permanent magnet, r is the distance from the origin, ω is the angular velocity and θ and ϕ are the angles between the $F_{\rm mag}$ and $F_{\rm radial}$ in the X-Y plane and Y-Z plane, respectively.

The magnetic force is calculated by taking the gradient of the magnetic energy density of the magnet volume element $F_{\rm mag} = \nabla U_{\rm mag}$. The instantaneous energy density of a magnetic field is given as

$$U_{\text{mag}} = \frac{1}{2} B \cdot H \tag{5}$$

where B is the magnetic induction and H is the magnetic field.

As is shown in Fig. 5B, depending on the rotation speed and the vertical distance between magnets, the equilibrium horizontal distance between magnets can be determined. For example, if the CD spins with the spin speed of 5 Hz and the vertical distance between the magnets is 3 mm, the magnetic force wins over the centrifugal force when the horizontal distance between the magnets is smaller than 3 mm. Above this distance the centrifugal force is larger than the magnetic force. Above a spin speed of 7 Hz, the centrifugal force is always larger than the magnetic force. Therefore, in our DNA extraction CD, the magnet is moved to the lysis chamber position when the CD was rotated with high speed, e.g., 10 Hz.

4. Conclusions

By combining the TS-LIMBS method with the novel LIFM and centrifugal microfluidics, we could, for the first time, fully integrate the complex microfluidic operational steps, such as specific virus DNA extraction from whole blood, on a CD. Furthermore, a portable device equipped with a small laser diode and CD mounting stage like a CD player was developed.

The TS-LIMBS method is advantageous because it is capable of target specific cell separation and concentration from raw samples, and DNA extraction and protein removal could be carried out in a short time without the requirement of the large volume of lysis buffer.

In the present report we have only demonstrated pathogen DNA extraction from whole blood on a CD. However, many other kinds of novel biological assays, *e.g.*, RNA preparation for cancer marker tests, molecular diagnostics of infectious diseases, genomic DNA preparation, various kinds of immunoassays, and blood chemistry analysis *etc.*, are also possible using the same centrifugal microfluidics with the novel LIFM control.

Acknowledgements

We would like to acknowledge Professor Marc Madou and Dr. Horacio Kido at the University of California at Irvine for technical consultations regarding the CD fabrication method using double sided tape bonding and the set-up of the test vehicle for the visualization of centrifugal microfluidics. We also thank Dr. Jung-Suk Yoo, Do-Kyoung Lee and Sungwoo Hong for helpful discussions and technical assistance. This research was sponsored in part by the Ministry of Commerce, Industry and Energy (MOCIE) of the Republic of Korea under the next generation new technology development project (00008069) through the Bio Device Research Lab at the Samsung Advanced Institute of Technology (SAIT).

References

- N. G. A. Manz and H. M. Widmer, Sens. Actuators, B, 1990, 1, 244–248.
- 2 A. J. de Mello, Nature, 2006, 442, 394-402.
- 3 G. M. Whitesides, Nature, 2006, 442, 368-373.
- 4 P. Yager, T. Edwards, E. Fu, K. Helton, K. Nelson, M. R. Tam and B. H. Weigl, *Nature*, 2006, 442, 412–418.
- D. Janasek, J. Franzke and A. Manz, *Nature*, 2006, 442, 374–380.
- 6 T. M. Squires and S. R. Quake, Rev. Mod. Phys., 2005, 77, 977–1026.
- 7 A. J. Tudos, G. A. J. Besselink and R. B. M. Schasfoort, *Lab Chip*, 2001, 1, 83–95.
- 8 D. Reyes, D. Iossifidis, P. Auroux and A. Manz, *Anal. Chem.*, 2002, 74, 2623–2636.
- 9 R. E. Oosterbroek and A. van den Berg, Lab-on-a-Chip: Miniaturized Systems for (Bio)chemical Analysis and Synthesis, Elsevier Science, Amsterdam, 2003.
- T. Vilkner, D. Janasek and A. Manz, *Anal. Chem.*, 2004, 76, 3373–3386.
- 11 D. I. P.-A. Auroux, D. R. Reyes and A. Manz, *Anal. Chem.*, 2002, 74, 2637–2652.
- 12 H. A. Stone, A. D. Stroock and A. Ajdari, Annu. Rev. Fluid Mech., 2004, 36, 381–411.
- 13 M. Toner and D. Irimia, Annu. Rev. Biomed. Eng., 2005, 7,
- 14 D. Figeys and D. Pinto, Anal. Chem., 2000, 72, 330-335.

- 15 R. H. Liu, J. Yang, R. Lenigk, J. Bonanno and P. Grodzinski, Anal. Chem., 2004, 76, 1824–1831.
- 16 J.-G. Lee, K. H. Cheong, N. Huh, S. Kim, J.-W. Choi and C. Ko, Lab Chip, 2006, 6, 886–895.
- 17 M. Madou and G. Kellogg, Proc. SPIE, 1998, 80-93.
- 18 M. Madou, Y. Lu, S. Lai, J. Lee and S. Daunert, *Proc. MicroTAS*, 2000, 565–570.
- 19 J. V. Zoval and M. J. Madou, Proc. IEEE, 2004, 92, 140-153.
- 20 D. C. Duffy, H. L. Gillis, J. Lin, N. F. Sheppard and G. J. Kellogg, Anal. Chem., 1999, 71, 4669–4678.
- 21 G. Ekstrand, C. Holmquist, A. E. Orleforn, B. Hellmann, A. Larsson and P. Andersson, *Proc. MicroTAS*, 2000, 311–314.
- 22 S. Lai, S. Wang, J. Luo, L. J. Lee, S.-T. Yang and M. J. Madou, Anal. Chem., 2004, 76, 1832–1837.
- 23 G. J. Kellogg, T. E. Arnold, B. L. Carvalho, D. C. Duffy and N. F. Sheppard, *Proc. MicroTAS*, 2000, 239–242.
- 24 M. Grumann, A. Geipel, L. Riegger, R. Zengerle and J. Ducree, *Lab Chip*, 2005, 5, 560–565.
- T. Brenner, T. Glatzel, R. Zengerle and J. Ducree, *Lab Chip*, 2005, 5, 146–150.
- S. Haeberle, T. Brenner, R. Zengerle and J. Ducree, *Lab Chip*, 2006, 6, 776–781.
- 27 R. D. Johnson, I. H. A. Badr, G. Barrett, S. Lai, Y. Lu, M. J. Madou and L. G. Bachas, *Anal. Chem.*, 2001, 73, 3940–3946.
- 28 L. G. Puckett, E. Dikici, S. Lai, M. Madou, L. G. Bachas and S. Daunert, *Anal. Chem.*, 2004, **76**, 7263–7268.

- 29 N. Honda, U. Lindberg, P. Andersson, S. Hoffmann and H. Takei, Clin. Chem., 2005, 51, 1955–1961.
- 30 J. Kim, S. H. Jang, G. Jia, J. V. Zoval, N. A. D. Silva and M. J. Madou, *Lab Chip*, 2004, 4, 516–522.
- 31 J. Steigert, M. Grumann, T. Brenner, L. Riegger, J. Harter, R. Zengerle and J. Ducree, *Lab Chip*, 2006, 6, 1040–1044.
- 32 M. Gustafsson, D. Hirschberg, C. Palmberg, H. Jornvall and T. Bergman, *Anal. Chem.*, 2004, **76**, 345–350.
- 33 C. T. Schembri, V. Ostoich, P. J. Lingane, T. L. Burd and S. N. Buhl, *Clin. Chem.*, 1992, 38, 1665–1670.
- 34 G. T. Schembri, T. L. Burd, A. R. Kopf-Sill, L. R. Shea and R. Braynin, J. Autom. Chem., 1995, 17, 99–104.
- 35 J.-M. Park, Y.-K. Cho, B.-S. Lee, J.-G. Lee and C. Ko, *Lab Chip*, 2007, DOI: 10.1039/b616112j.
- 36 G. Kellogg, S. G. Kieffer-Higgins, B. L. Carvalho, G. A. Davis, J. P. Willis, T. Minior, L. L. Chapman, M. Kob, S. D. Oeltjen, S. Ommert and A. Mian, in 'Devices and methods for using centripetal acceleration to drive fluid movement on a microfluidics system', US 6063589, May 16, 2000.
- 37 K. W. Oh and C. H. Ahn, J. Micromech. Microeng., 2006, 16, R13–R39.
- 38 Y.-K. Cho, J. Kim, Y. Lee, Y.-A. Kim, K. Namkoong, H. Lim, K. W. Oh, S. Kim, J. Han, J. Park, Y. E. Pak, C.-S. Ki, J. R. Choi, H.-K. Myeong and C. Ko, *Biosens. Bioelectron.*, 2006, 21, 2161–2169.
- 39 R. W. Chen, H. Piiparinen, M. Seppanen, P. Koskela, S. Sarna and M. Lappalainen, *J. Med. Virol.*, 2001, **65**, 250–256.